

EFFECTS OF A PULSATILE FLOW AND AN ENDOSCOPE ON THE PERISTALTIC TRANSPORT OF A NEWTONIAN FLUID

H. RACHID[†], M.T. OUAZZANI, M. RIAHI

Department of Physics, Faculty of Sciences Ain Chock, University Hassan II
Maarif, Casablanca 5366, Morocco

(Received March 23, 2015; revised version received May 13, 2015)

This article analytically investigates the effect of pulsatile flow on the peristaltic transport of a Newtonian fluid between two coaxial cylinders. The inner tube is rigid and uniform and the outer tube has a sinusoidal wave traveling down its wall. This transport is studied under low Reynolds number and long wavelength approximations. The governing equations are developed up to the second order in the Womersley number. We first analyzed the effects of the Womersley, the amplitude ratio and the radius ratio on the pressure rise and on the frictional forces. The instantaneous mechanical efficiency of pumping phenomenon has been graphically presented and the influence of physical parameters on this efficiency has been studied.

DOI:10.5506/APhysPolB.46.2051

PACS numbers: 47.85.-g, 47.15.G-, 87.19.rh

1. Introduction

Peristaltic pumping is a mechanism of fluid transport in a flexible tube by a progressive wave of contraction or expansion from a region of lower pressure to higher pressure. These movements of the walls propel the fluid. Peristalsis is one of the major mechanisms for fluid in many biological systems. It is an automatic and vital process that moves food through the digestive tract. The blood flow in the human body is another major application of peristaltic pumping. The description of the phenomenon associated to this transport has been studied by many authors. The first investigation was by Latham [1] and Jaffrin and Shapiro [2]. Later, the non-Newtonian effects of fluids without endoscope [3–6] or with endoscope [7–15] was the aim of the majority of studies. In all these works, the authors supposed that the flow in the wave frame is steady and the associated phenomenon

[†] Corresponding author: rhassan2@yahoo.fr

is due to the dynamic interaction between the flow of fluid and the motion in space of the wall of the tube. But when the fluid is pulsatile, the flow in the wave frame becomes unsteady. Despite its importance, due to the complexity of the time-dependent problems, we find in the literature just a few articles which attempted to study the effect of pulsatile flow on peristaltic transport and without endoscope. For example, Segesser *et al.* [16] studied the peristaltic effect and the pulsatile flow of an Arthropump. Usha and Prema [17] analyzed interaction of pulsatile and peristaltic transport induced flows of a particle–fluid suspension. Kumar and Prasad [18] analyzed the peristaltic and pulsatile flow of a couple stress fluid through porous medium in a channel bounded by flexible walls. Srivastava [19] studied the interaction of peristaltic transport with pulsatile flow of a Newtonian viscous incompressible fluid in a circular cylindrical tube. Afifi and Gad studied the interaction of peristaltic flow with pulsatile flow for a magneto-fluid [20] or for a viscous incompressible fluid through a porous medium [21]. Gad [22] investigates the effect of Hall currents on interaction of pulsatile and peristaltic transport induced flows of a particle–fluid suspension. In the last four works, the authors supposed that the frequency of the traveling wave and that of the imposed pressure gradient are equal. In addition, they analyzed only the effect of interest parameters on the velocity in the time independent case (steady flow).

Therefore, the aim of the present paper is to analytically investigate the effect of pulsatile flow on peristaltic transport between two coaxial tubes. The inner tube is rigid and uniform and the outer tube has sinusoidal waves traveling down its walls. Here, we suppose that the imposed pressure gradient is a function periodic in time whose frequency is different from that of the traveling wave of the outer tube. The problem is simplified under long wavelength and low Reynolds number approximations to obtain the expressions of the instantaneous pressure gradient. The influence of pulsatile flow and the effect of different physical parameters on the instantaneous pressure rise, frictional forces and on the instantaneous mechanical efficiency of pumping are shown graphically and discussed.

2. Formulation and analysis

We consider the unsteady peristaltic transport of a Newtonian fluid flowing between two coaxial cylinders. The geometry of the walls surfaces (*cf.* Fig. 1) is:

$$\bar{r}_1 = a_1, \quad (1)$$

$$\bar{r}_2 = \bar{H}(\bar{Z}, \bar{t}) = a_2 + b \cos\left(\frac{2\pi}{\lambda}(\bar{Z} - c\bar{t})\right), \quad (2)$$

where a_1 and a_2 are the radii of the inner and outer tubes at inlet, b is the wave amplitude of the outer tube, λ is the wavelength, c is the propagation velocity, \bar{t} is the time. We choose a cylindrical coordinate system (\bar{R}, \bar{Z}) where the \bar{Z} -axis lies along the centerline of the inner and the outer tubes, and the \bar{R} -axis is transverse to it.

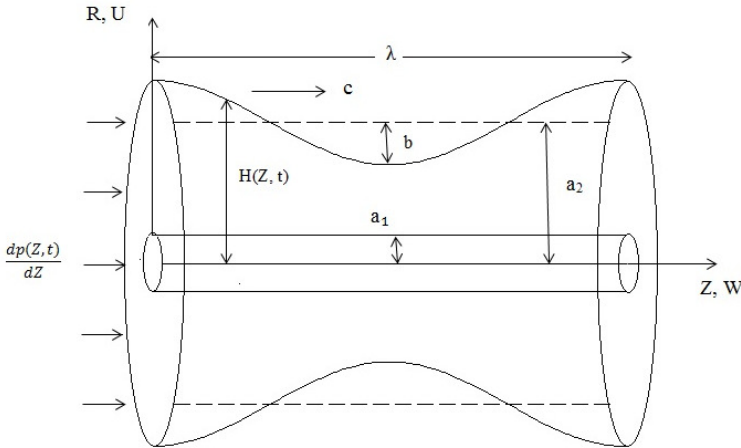


Fig. 1. Geometry of the problem.

The equations of motion of the flow in the gap between the inner and the outer tubes are:

$$\rho \left[\frac{\partial \bar{U}}{\partial \bar{t}} + \bar{U} \frac{\partial \bar{U}}{\partial \bar{R}} + \bar{W} \frac{\partial \bar{U}}{\partial \bar{Z}} \right] = - \frac{\partial \bar{p}}{\partial \bar{R}} + \mu \frac{\partial}{\partial \bar{R}} \left(\frac{1}{\bar{R}} \frac{\partial (\bar{R}\bar{U})}{\partial \bar{R}} \right) + \mu \frac{\partial^2 \bar{U}}{\partial \bar{Z}^2}, \quad (3)$$

$$\rho \left[\frac{\partial \bar{W}}{\partial \bar{t}} + \bar{U} \frac{\partial \bar{W}}{\partial \bar{R}} + \bar{W} \frac{\partial \bar{W}}{\partial \bar{Z}} \right] = - \frac{\partial \bar{p}}{\partial \bar{Z}} + \mu \frac{1}{\bar{R}} \frac{\partial}{\partial \bar{R}} \left(\bar{R} \frac{\partial \bar{W}}{\partial \bar{R}} \right) + \mu \frac{\partial^2 \bar{W}}{\partial \bar{Z}^2}, \quad (4)$$

$$\frac{\partial \bar{U}}{\partial \bar{R}} + \frac{\bar{U}}{\bar{R}} + \frac{\partial \bar{W}}{\partial \bar{Z}} = 0, \quad (5)$$

where ρ is the fluid density, \bar{U} and \bar{W} are the velocity components in the laboratory frame and \bar{p} is the pressure.

The system coordinates in the laboratory frame and the wave frame are related through

$$\bar{z} = \bar{Z} - c\bar{t}; \quad \bar{r} = \bar{R} \quad (6)$$

and the velocity components are also related by

$$\bar{u}(\bar{r}, \bar{z}) = \bar{U}(\bar{R}, \bar{Z} - c\bar{t}); \quad \bar{w}(\bar{r}, \bar{z}) = \bar{W}(\bar{R}, \bar{Z} - c\bar{t}) - c, \quad (7)$$

where \bar{u} and \bar{w} are the velocity components in the wave frame.

The boundary conditions are:

$$\bar{u} = 0, \quad \bar{w} = -c \quad \text{at} \quad \bar{r} = \bar{r}_1, \tag{8}$$

$$\bar{u} = -c \frac{d\bar{r}_2}{d\bar{z}}, \quad \bar{w} = -c \quad \text{at} \quad \bar{r} = \bar{r}_2. \tag{9}$$

For carrying out further analysis, we introduce the following dimensionless parameters:

$$\begin{aligned} z &= \frac{\bar{z}}{\lambda}; & r_1 &= \varepsilon = \frac{\bar{r}_1}{a_2}; & r_2 &= \frac{\bar{r}_2}{a_2}; & t &= \frac{\bar{t}}{T_0}; & u &= \frac{\lambda \bar{u}}{a_2 c}; \\ w &= \frac{\bar{w}}{c}; & p &= \frac{a_2^2 \bar{p}}{\mu \lambda c}; & Q &= \frac{\bar{Q}}{\pi c a_2^2}; & \delta &= \frac{a_2}{\lambda}; & \beta &= \frac{\rho a_2^2}{\mu T_0}; \\ R_e &= \frac{\rho c a_2}{\mu}; & \varepsilon &= \frac{a_1}{a_2}; & \phi &= \frac{b}{a_2}, \end{aligned} \tag{10}$$

where T_0 is the characteristic time related to the imposed periodic pressure gradient, δ is the dimensionless wave number, β is the Womersley number, R_e is the Reynolds number, ε is the radius ratio and ϕ is the amplitude ratio of the outer tube, where $0 < \phi < 1 - \varepsilon$.

After defining the dimensionless stream function $\psi(r, z)$ given by

$$u(r, z) = -\frac{1}{r} \frac{\partial \psi}{\partial z}; \quad w(r, z) = \frac{1}{r} \frac{\partial \psi}{\partial r}, \tag{11}$$

and using the above non-dimensional quantities, the continuity equation is satisfied and the equations of motion (5) become:

$$\begin{aligned} & -\delta^2 \beta \frac{\partial}{\partial t} \left(\frac{1}{r} \frac{\partial \psi}{\partial z} \right) + R_e \delta^3 \left(\frac{1}{r} \frac{\partial \psi}{\partial z} \frac{\partial}{\partial r} - \frac{1}{r} \frac{\partial \psi}{\partial r} \frac{\partial}{\partial z} \right) \frac{1}{r} \frac{\partial \psi}{\partial z} \\ &= -\frac{\partial p}{\partial r} - \delta^2 \frac{1}{r} \frac{\partial}{\partial r} \left(r \frac{\partial}{\partial r} \left(\frac{1}{r} \frac{\partial \psi}{\partial z} \right) \right) - \delta^4 \frac{\partial}{\partial z} \left(\frac{\partial}{\partial z} \left(\frac{1}{r} \frac{\partial \psi}{\partial z} \right) \right), \\ & \beta \frac{\partial}{\partial t} \left(\frac{1}{r} \frac{\partial \psi}{\partial r} \right) - R_e \delta \left(\frac{1}{r} \frac{\partial \psi}{\partial z} \frac{\partial}{\partial r} - \frac{1}{r} \frac{\partial \psi}{\partial r} \frac{\partial}{\partial z} \right) \frac{1}{r} \frac{\partial \psi}{\partial r} \\ &= -\frac{\partial p}{\partial z} + \frac{1}{r} \frac{\partial}{\partial r} \left(r \frac{\partial}{\partial r} \left(\frac{1}{r} \frac{\partial \psi}{\partial r} \right) \right) + \delta^2 \frac{\partial}{\partial z} \left(\frac{\partial}{\partial z} \left(\frac{1}{r} \frac{\partial \psi}{\partial r} \right) \right). \end{aligned} \tag{12}$$

3. Volume flow rate and boundary conditions

The volume rate of flow in the fixed coordinate system (\bar{R}, \bar{Z}) is given as:

$$\bar{Q}(\bar{Z}, \bar{t}) = 2\pi \int_{\bar{r}_1}^{\bar{r}_2} \bar{W}(\bar{Z}, \bar{t}) \bar{R} d\bar{R}. \tag{13}$$

Substituting (6) and (7) in (13), we obtain

$$\bar{Q}(\bar{Z}, \bar{t}) = \bar{q}(\bar{t}) + \pi c (\bar{r}_2^2 - \bar{r}_1^2), \tag{14}$$

where

$$\bar{q}(\bar{t}) = 2\pi \int_{\bar{r}_1}^{\bar{r}_2} \bar{w} \bar{r} \, d\bar{r} \tag{15}$$

is the volume flow rate in the moving coordinate system.

The space-mean flow over a wavelength is defined by

$$\bar{Q}(\bar{t}) = \frac{1}{\lambda} \int_0^\lambda \bar{Q}(\bar{Z}, \bar{t}) \, d\bar{Z}. \tag{16}$$

Substituting (14) in (16), we find

$$\bar{Q}(\bar{t}) = \bar{q}(\bar{t}) + \pi c a_2^2 \left(1 + \frac{\phi^2}{2} - \varepsilon^2 \right). \tag{17}$$

Using dimensionless variables, we obtain

$$\theta(t) = q(t) + \left(1 + \frac{\phi^2}{2} - \varepsilon^2 \right) \tag{18}$$

with

$$\theta(t) = \frac{\bar{Q}(\bar{t})}{\pi c a_2^2}, \tag{19}$$

$$q(t) = \frac{\bar{q}(\bar{t})}{\pi c a_2^2} = 2 \int_\varepsilon^{r_2} \frac{\partial \psi}{\partial r} \, dr = 2 [\psi(r_2) - \psi(\varepsilon)]. \tag{20}$$

The corresponding dimensionless boundary conditions in the wave frame are given by:

$$\psi(\varepsilon) = 0; \quad \frac{1}{r} \frac{\partial \psi}{\partial r} \Big|_{r=\varepsilon} = -1, \tag{21}$$

$$\psi(r_2) = \frac{q(t)}{2}; \quad \frac{1}{r} \frac{\partial \psi}{\partial r} \Big|_{r=r_2} = -1. \tag{22}$$

Under the assumptions of long wavelength approximation (*i.e.*, $\lambda \gg a_2$) and low Reynolds number (*i.e.*, $Re \rightarrow 0$), Eqs. (12) can be reduced to:

$$\begin{aligned} \frac{\partial p}{\partial r} &= 0, \\ \beta \frac{\partial}{\partial t} \left(\frac{1}{r} \frac{\partial \psi}{\partial r} \right) &= -\frac{\partial p}{\partial z} + \frac{1}{r} \frac{\partial}{\partial r} \left(r \frac{\partial}{\partial r} \left(\frac{1}{r} \frac{\partial \psi}{\partial r} \right) \right) \end{aligned} \tag{23}$$

and the boundary conditions are the same as given by Eqs. (21)–(22).

4. Method of solution

In this work, we recall that the flow is unsteady even in the wave frame analysis because of the existence of a pulsatile flow. We also assume that the flow rate $F(t)$ in this frame is given by

$$q(t) = q_0 + \beta q_1(t), \tag{24}$$

where q_0 is the flow rate in the wave frame in the absence of the pulsatile flow and $q_1(t)$ is a function of time of frequency ω_2 . Taking into account this assumption, the characteristic time T_0 mentioned in (10) is related to the dimensional flow rate $\bar{q}(t)$ and is given by [23]

$$\frac{1}{T_0} = \text{Max} \left| \frac{1}{\bar{q}(\bar{t})} \frac{\partial \bar{q}(\bar{t})}{\partial \bar{t}} \right| = \frac{\omega_2}{2\pi}. \tag{25}$$

Therefore, we seek the solution of the problem under small Womersley number β , we expand ψ and p in the following form:

$$\begin{aligned} \psi &= \psi_0 + \beta \psi_1 + \beta^2 \psi_2 + \dots, \\ p &= p_0 + \beta p_1 + \beta^2 p_2 + \dots \end{aligned} \tag{26}$$

substituting (24) and (26) into (23) and (21)–(22), summing up the different orders of solution, we obtain

$$\begin{aligned} \frac{\partial p(z, t)}{\partial z} &= 8 \left(\frac{\left(\theta(t) - \int_0^1 (r_2^2 - \varepsilon^2) dz + (r_2^2 - \varepsilon^2) \right) \ln \left(\frac{r_2}{\varepsilon} \right)}{(r_2^2 - \varepsilon^2)^2 - (r_2^4 - \varepsilon^4) \ln \left(\frac{r_2}{\varepsilon} \right)} \right) \\ &+ \beta \left(\frac{2 (r_2^2 - \varepsilon^2) + 3 (r_2^4 - \varepsilon^4) \ln \left(\frac{r_2}{\varepsilon} \right) - \frac{4}{3} (r_2^4 + \varepsilon^4 + r_2^2 \varepsilon^2) \ln \left(\frac{r_2}{\varepsilon} \right)^2}{(r_2^2 - \varepsilon^2) \left[(r_2^2 - \varepsilon^2)^2 - (r_2^4 - \varepsilon^4) \ln \left(\frac{r_2}{\varepsilon} \right) \right]} \right) \frac{d\theta(t)}{dt}. \end{aligned} \tag{27}$$

For $\beta = 0$, the pressure gradient (27) becomes the same as given in Eqs. (3)–(8) by Hayat *et al.* [24] or by Mekheimer [25] where they take the non-uniform parameter of the channel $k = 0$ and the velocity parameter of endoscope $V_0 = 0$.

5. The pumping characteristics

The instantaneous pressure rise $\Delta p(t)$ and frictional forces at the walls of the inner and the outer tubes $F^{(i)}(t)$ and $F^{(o)}(t)$, in the non-dimensional form, are given by

$$\Delta p(t) = \int_0^1 \frac{\partial p(z, t)}{\partial z} dz, \tag{28}$$

$$F^{(o)}(t) = \int_0^1 r_2^2 \left(-\frac{\partial p(z, t)}{\partial z} \right) dz, \tag{29}$$

$$F^{(i)}(t) = \int_0^1 \varepsilon^2 \left(-\frac{\partial p(z, t)}{\partial z} \right) dz. \tag{30}$$

6. Instantaneous mechanical efficiency of pumping

The mechanical efficiency is defined as the ratio between the average rate per wavelength at which work is done by the moving fluid against a pressure head and the average rate at which the walls do work on the fluid [26–28].

It is given by

$$E(t) = \frac{\mathcal{P}_{s_1} + \mathcal{P}_{s_2}}{\mathcal{P}_1 + \mathcal{P}_2}, \tag{31}$$

where \mathcal{P}_1 and \mathcal{P}_2 are the works provided by the walls of the inner and outer tubes, respectively. \mathcal{P}_{s_1} and \mathcal{P}_{s_2} are the powers developed on the section s_1 of abscissa $Z_1 = 0$ and on the section s_2 of abscissa $Z_2 = \lambda$, respectively.

When we neglect the friction forces, the work $\mathcal{P}_1 + \mathcal{P}_2$ is given by

$$\mathcal{P}_1 + \mathcal{P}_2 = \int_{S_1} \vec{T}_1 \vec{V} dS_1 + \int_{S_2} \vec{T}_2 \vec{V} dS_2, \tag{32}$$

where \vec{T}_1 and \vec{T}_2 are the forces exercised by the walls (of lateral surfaces S_1 of the inner tube and S_2 of the outer tube) on the fluid. \vec{V} is the vector velocity.

In the fixed frame, we obtain $\mathcal{P}_1 + \mathcal{P}_2$ as

$$\mathcal{P}_1 + \mathcal{P}_2 = -2\pi \int_0^1 p_{\text{wall}} (r_2 - \varepsilon) \frac{\partial (r_2 - \varepsilon)}{\partial t} dZ, \tag{33}$$

where p_{wall} is the pressure on the walls.

The energy useful for the pumping of fluid $\mathcal{P}_{s_1} + \mathcal{P}_{s_2}$ is defined as

$$\mathcal{P}_{s_1} + \mathcal{P}_{s_2} = \int_{s_1} \vec{f}_1 \vec{V} ds_1 + \int_{s_2} \vec{f}_2 \vec{V} ds_2, \tag{34}$$

where \vec{f}_1 and \vec{f}_2 are the forces exercised on the fluid at the sections s_1 and s_2 , respectively. We find:

$$\mathcal{P}_{s_1} + \mathcal{P}_{s_2} = 2\pi p(0, t) \int_{\varepsilon}^{r_2} W(r, 0, t)r dr - 2\pi p(1, t) \int_{\varepsilon}^{r_2} W(r, 1, t)r dr \quad (35)$$

or

$$\mathcal{P}_{s_1} + \mathcal{P}_{s_2} = \pi [p(0, t) Q(0, t) - p(1, t) Q(1, t)] . \quad (36)$$

The flow rate $Q(Z, t)$ is periodic in the space, thus we obtain

$$\mathcal{P}_{s_1} + \mathcal{P}_{s_2} = -\pi \Delta p(t) Q(0, t) . \quad (37)$$

The instantaneous mechanical efficiency becomes

$$E(t) = \frac{\Delta P(t) Q(0, t)}{2 \int_0^1 P_{\text{wall}} (r_2 - \varepsilon) \frac{\partial(r_2 - \varepsilon)}{\partial t} dZ} . \quad (38)$$

After simple integration, we find

$$E(t) = \frac{-Q(0, t)\Delta p(t)}{\Omega (\Delta p(t) [r_2^2(0) - \varepsilon^2] + F^{(o)}(t) + F^{(i)}(t) + 2I)} , \quad (39)$$

where $I = \int_0^1 \varepsilon r_2 \frac{\partial p(z, t)}{\partial z} dz$, $\Omega = \frac{\omega_1}{\omega_2} = \frac{T_0 c}{\lambda}$ is the reduced frequency. $Q(0, t)$ is the flow rate in the fixed frame at $Z = 0$, and is given by

$$Q(0, t) = \theta(t) + r_2^2(0, t) - \left(1 + \frac{\phi^2}{2}\right) . \quad (40)$$

We notice that for $\varepsilon = 0$, Eq. (39) becomes the same Eq. (33) found by Rachid and Ouazzani [29] where they take the Deborah number $D_b = 0$.

7. Results and discussions

In this section we analyze the effects of the Womersley number β , the amplitude ration ϕ and the radius ration ε on the pressure rise Δp , frictional forces $F^{(i)}$ and $F^{(o)}$ and on the instantaneous mechanical efficiency $E(t)$. In this investigation, the flow is unsteady even in the wave frame due to the existence of an imposed pressure gradient variable in time. Here, we suppose that the flow rate $\theta(t)$ is given by [29]

$$\theta(t) = \theta_0 + \beta \sin(2\pi t) . \quad (41)$$

7.1. Pressure rise

We notice that for $\beta = 0$, the flow is steady in the wave frame because the flow rate θ is independent of time and Eq. (41) becomes $\theta = \theta_0$. In this case, the relations pressure rise flow rate $\Delta p-\theta$ and frictional forces-flow rate $F-\theta$ are straight lines. In addition, for $\varepsilon = 0$, we find the classical results of peristaltic transport of a Newtonian fluid without endoscope [28]. The results of Mekheimer [25] can be recovered when he takes $V_0 = 0$. In Fig. 2 (curve D), we plot the pressure rise *versus* the flow rate for the steady case and for $\phi = 0.4$ and $\varepsilon = 0.2$.

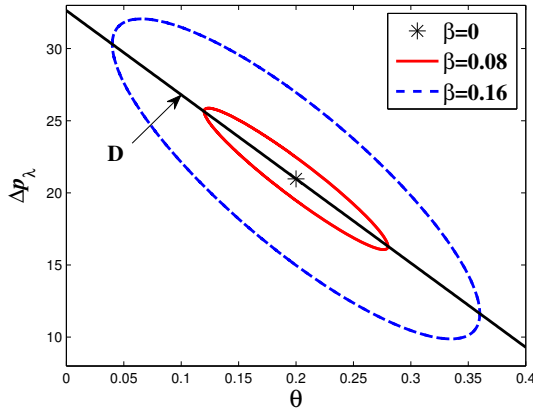


Fig. 2. Pressure rise Δp *versus* flow rate θ for different values of β with $\phi = 0.4$, $\varepsilon = 0.2$ and $\theta_0 = 0.2$.

In the presence of pulsatile flow ($\beta \neq 0$), the flow becomes unsteady even in the wave frame. In Fig. 2, we also plot the pressure rise Δp *versus* the flow rate θ for $\phi = 0.4$, $\varepsilon = 0.2$, for a given value of the flow rate θ_0 (abscissa of one point of the curve D) and for different values of the Womersley number β . We observe that Δp becomes ellipses because of the existence of the term $d\theta(t)/t$ in the expression of the pressure gradient (27) and the variation of time in Eq. (41) which generates the variation of the flow rate $\theta(t)$. The same figure shows that the lengths of the principal and of the minor axis of the ellipses change in the direction of the principal axis with the increase in β .

In Figs. 3 (a), (b) we plot the pressure rise Δp *versus* flow rate θ for different values of the amplitude ratio ϕ and the radius ratio ε , respectively, for a given value of the flow rate θ_0 and Womersley number β . These figures show that the distribution of Δp is always ellipses whose length of the minor axis increases with the increase in ϕ and ε with a change in the

direction of the principal axis. In addition, these figures indicate that the peristaltic pumping region ($\Delta p > 0$ and $\theta > 0$) increases with increasing ϕ and ε .

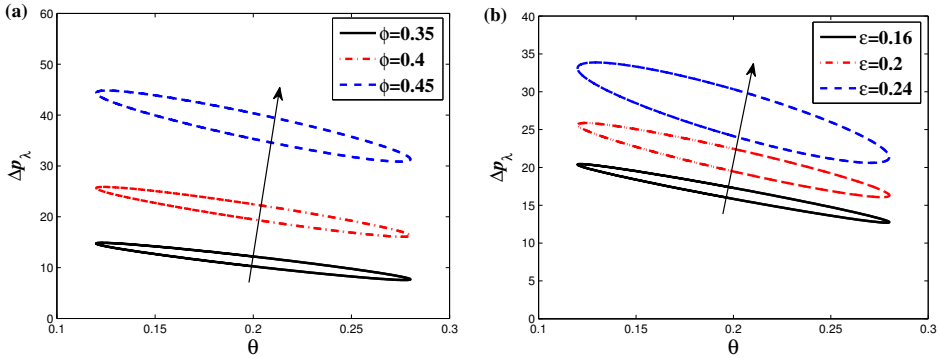


Fig. 3. Pressure rise Δp versus flow rate θ with $\beta = 0.08$ and $\theta_0 = 0.2$ for: (a) different values of ϕ with $\varepsilon = 0.2$ (b) different values of ε with $\phi = 0.4$.

In Fig. 4, we present the instantaneous pressure rise $\Delta p(t)$ versus time for different values of the Womersley number β . This figure shows that for $\beta = 0$, the pressure rise Δp is constant but for $\beta \neq 0$ Δp becomes periodic and sinusoidal in time and the amplitude of the sinusoid increases with the increase in β .

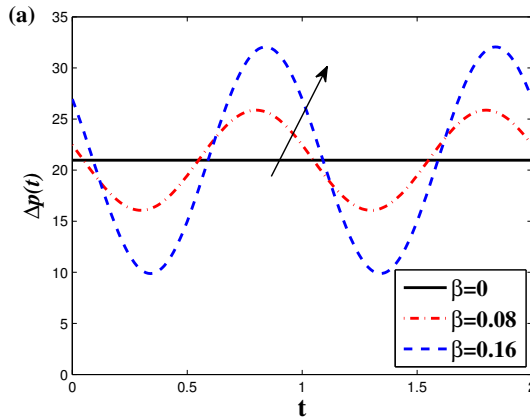


Fig. 4. Instantaneous pressure rise $\Delta p(t)$ versus time t for different values of β with $\phi = 0.4$, $\varepsilon = 0.2$ and $\theta_0 = 0.2$.

For different values of ϕ and ε , the instantaneous pressure rise $\Delta p(t)$ is plotted in Fig. 5. From this figure, it can be seen that $\Delta p(t)$ and its amplitude increase together with increasing ϕ and ε .

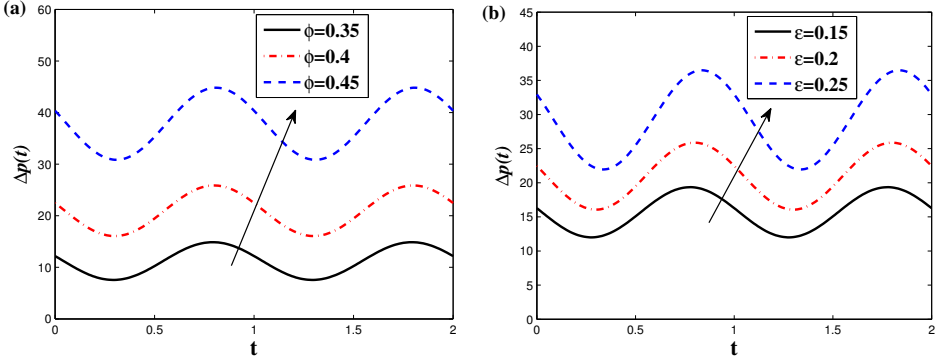


Fig. 5. Instantaneous pressure rise $\Delta p(t)$ versus time t corresponding to (a) different values of ϕ with $\varepsilon = 0.2$, (b) different values of ε with $\phi = 0.4$.

7.2. Frictional forces

In Figs. 6 (a), (b), we represent the frictional forces on the inner tube $F^{(i)}$ and on the outer tube $F^{(o)}$, respectively, versus the flow rate θ for different values of the Womersley β with $\phi = 0.4$, $\varepsilon = 0.2$, $\theta_0 = 0.2$. These figures show that $F^{(i)}$ and $F^{(o)}$ have an opposite behavior to the pressure rise and the curves are also ellipses with the same remarks as in Fig. 2.

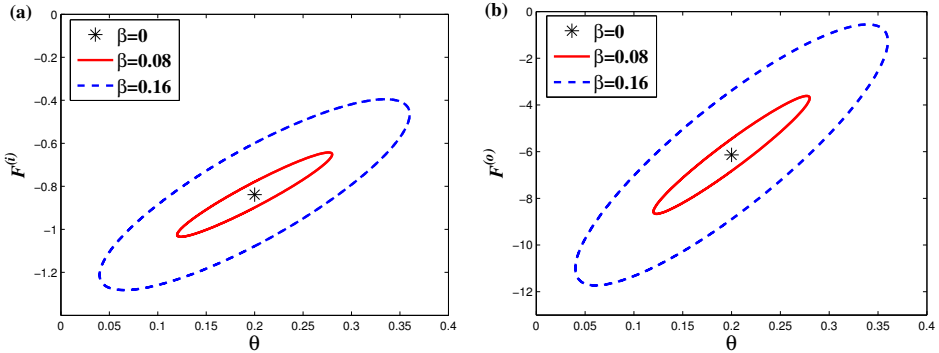


Fig. 6. Frictional forces on the inner tube $F^{(i)}$ (a) and on the outer tube $F^{(o)}$ (b) versus the flow rate θ for different values of β with $\phi = 0.4$, $\varepsilon = 0.2$ and $\theta_0 = 0.2$.

Figs. 7–8 display the frictional forces $F^{(i)}$ and $F^{(o)}$ versus the flow rate θ for different values of the amplitude ratio ϕ and the radius ratio ε , respectively. These figures show that $F^{(i)}$ and $F^{(o)}$ have an opposite behavior to the pressure rise Δp with increasing ϕ and ε with the same observations as in Figs. 3 (a), (b). In addition, Figs. 6–8 indicate that the frictional force on the outer tube $F^{(o)}$ is greater than the frictional force on the inner tube $F^{(i)}$ for the same values of the physical parameters.

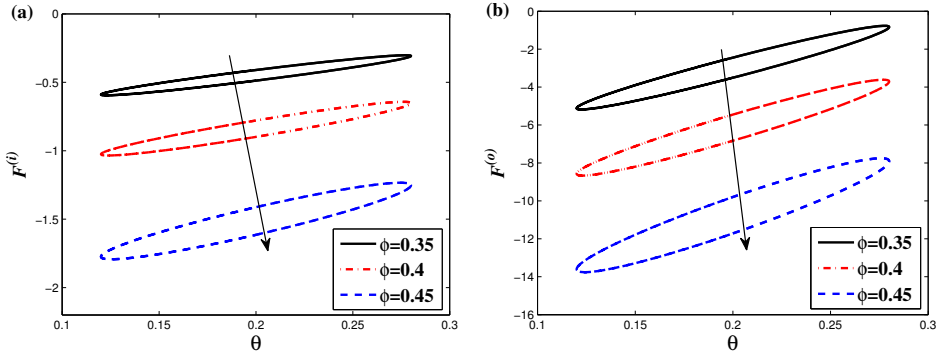


Fig. 7. Frictional forces on the inner tube $F^{(i)}$ (a) and on the outer tube $F^{(o)}$ (b) versus the flow rate θ for different values of ϕ with $\beta = 0.08$, $\varepsilon = 0.2$ and $\theta_0 = 0.2$.

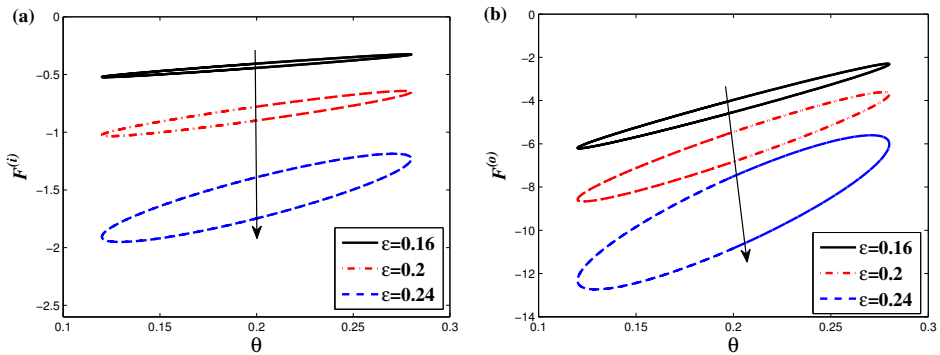


Fig. 8. Frictional forces on the inner tube $F^{(i)}$ (a) and on the outer tube $F^{(o)}$ (b) versus the flow rate θ for different values of ε with $\beta = 0.08$, $\phi = 0.4$ and $\theta_0 = 0.2$.

7.3. Instantaneous mechanical efficiency

In Fig. 9, we display the instantaneous mechanical efficiency $E(t)$ versus time for different values of the reduced frequency Ω with $\beta = 0.13$, $\phi = 0.35$, $\varepsilon = 0.2$ and $\theta_0 = 0.1$. This figure indicates that for $\Omega = 1$ (*i.e.* the frequency of the peristaltic transport and that of the pulsatile flow are equal), the distribution of $E(t)$ is periodic and sinusoidal. But for $\Omega \neq 1$, $E(t)$ remains periodic but not sinusoidal. This figure also shows that there is a proportional relationship between Ω and the number of spikes (for $\Omega \geq 1$) whose amplitude decreases with the increase in Ω .

In order to analyze the effects of the other physical parameters on the instantaneous mechanical efficiency $E(t)$, we suppose that $\Omega = 1$. Figure 10 describes the distribution of $E(t)$ versus time for different values of the Womersley number β . It is concluded that $E(t)$ is always periodic whose

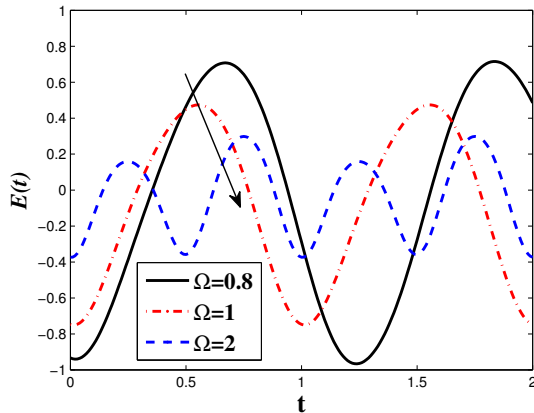


Fig. 9. Instantaneous mechanical efficiency $E(t)$ versus time t for different values of Ω with $\beta = 0.13$, $\phi = 0.35$, $\varepsilon = 0.2$ and $\theta_0 = 0.1$.

amplitude increases with increasing β . In addition, above a certain value of β , the effect of the second frequency linked to the pulsatile flow ($\omega_2 = \frac{2\pi}{T_0}$) on $E(t)$ appears clearly in the figure.

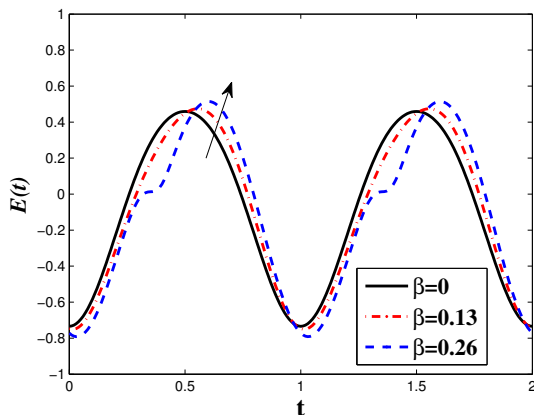


Fig. 10. Instantaneous mechanical efficiency $E(t)$ versus time t for different values of β with $\Omega = 1$, $\phi = 0.35$, $\varepsilon = 0.2$ and $\theta_0 = 0.1$.

In Figs. 11–12, we plot the instantaneous mechanical efficiency $E(t)$ versus time for different values of the amplitude ratio ϕ and the radius ratio ε , respectively. From these figures, it is observed that the amplitude of $E(t)$ increases with increasing ϕ and ε .

Finally, we note that in this modeling, all these results can constitute a control aid of the influence of pulsatile flow and the geometric effects on the peristaltic pumping phenomenon.

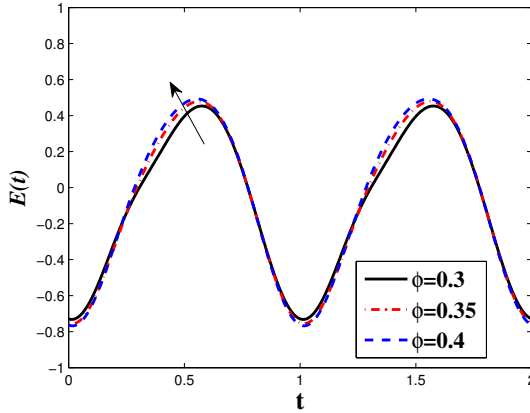


Fig. 11. Instantaneous mechanical efficiency $E(t)$ versus time t for different values of ϕ with $\Omega = 1$, $\beta = 0.13$, $\varepsilon = 0.2$ and $\theta_0 = 0.1$.

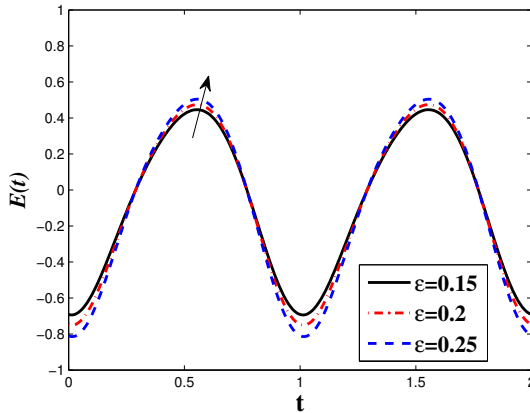


Fig. 12. Instantaneous mechanical efficiency $E(t)$ versus time t for different values of ε with $\Omega = 1$, $\beta = 0.13$, $\phi = 0.35$ and $\theta_0 = 0.1$.

8. Conclusions

In this investigation, we have analytically studied the interaction of pulsatile flow with peristaltic transport of a Newtonian fluid when a rigid uniform endoscope is inserted in a tube. The problem is simplified under the assumptions of long wavelength approximation and low Reynolds number. The analytical solution is obtained by an asymptotic method in terms of small Womersley number. The pressure rise, frictional forces and the instantaneous mechanical efficiency are discussed with the physical parameters, Womersley number β , the radius ratio ε and the amplitude ratio of the outer tube ϕ .

The graphical solutions have shown that:

1. The pressure rise Δp and the frictional forces $F^{(i)}$ and $F^{(o)}$ versus the flow rate θ are ellipses whose the principal and the median axis increase with increasing the Womersley number β .
2. The peristaltic pumping region increase with the increase in amplitude ratio ϕ and radius ratio ε .
3. The amplitude of the instantaneous pressure rise $\Delta p(t)$ increases with the increase in β .
4. $\Delta p(t)$ and his amplitude increase with increasing ϕ and ε .
5. An increase in the reduced frequency causes an increase of the number of spikes of the instantaneous mechanical efficiency $E(t)$ and a decrease of the amplitude of these spikes.
6. The amplitude of $E(t)$ increases with increasing β where the frequency of the linked to the pulsatile flow appears, in graph, above a certain value of β .
7. The amplitude of $E(t)$ increases with the increase in ϕ and ε .
8. For $\beta = 0$ (absence of pulsatile flow) and $\varepsilon = 0$ (without endoscope), we found the classical results of Shapiro *et al.* [28].
9. For $\varepsilon = 0$, the results of Rachid and Ouazzani [29] can be recovered when they take $D_b = 0$.
10. For $\beta = 0$, we obtain the same pressure gradient (3–8) of Hayat *et al.* [24] or of Mekheimer *et al.* [25] when they take $k = 0$ and $V_0 = 0$.

REFERENCES

- [1] T.W. Latham, M.S. Thesis, Massachusetts Institute of Technology, Cambridge 1966.
- [2] M.Y. Jaffrin, A.H. Shapiro, *Annu. Rev. Fluid Mech.* **3**, 13 (1971).
- [3] A.V. Mernone, J.N. Mazumdar, *Math. Comput. Model.* **35**, 895 (2002).
- [4] P. Muthu, B.V. Rathish Kumar, P. Chandra, *Appl. Math. Mod.* **32**, 2019 (2008).
- [5] A.M. Siddiqui, W.H. Schwarz, *J. Non-Newton. Fluid Mech.* **53**, 257 (1994).
- [6] D. Tripathi, P.K. Gupta, S. Das, *Thermal Science* **15**, 501 (2011).
- [7] A. Abd El Naby, A.E.M. El Misiery, *Appl. Math. Comput.* **128**, 19 (2002).

- [8] N.S. Akbar, S. Nadeem, *Commun. Theor. Phys.* **56**, 761 (2011).
- [9] N.S. Akbar, S. Nadeem, *Chin. Phys. B* **22**, 15201 (2013).
- [10] A.M. El Misery, Abd El Hakeem, Abd El Naby, A. El Nagar, *J. Phys. Soc. Jpn.* **72**, 89 (2003).
- [11] T. Hayat, N. Ali, *Math. Comput. Model.* **48**, 721 (2008).
- [12] K.S. Mekheimer, Y. Abd Elmaboud, *Phys. Lett. A* **372**, 1657 (2008).
- [13] K.S. Mekheimer, Y. Abd Elmaboud, *Physica A: Stat. Mech. Appl.* **387**, 2403 (2008).
- [14] S. Nadeem, N.S. Akbar, *Int. J. Numer. Meth. Fl.* **66**, 212 (2010).
- [15] V.P. Srivastava, *Appl. Appl. Math.* **2**, 79 (2007).
- [16] L. Von Segesser, A. Jeanjacquot, P. Meyer, J.B. Buchs, *J. Biomed. Eng.* **6**, 146 (1984).
- [17] R. Usha, K. Prema, *Z.A.M.M.* **78**, 207 (1998).
- [18] S.R. Kumar, R.S. Prasad, *Eur. J. Pure Appl. Math.* **3**, 213 (2010).
- [19] L.M. Srivastava, V.P. Srivastava, *J. Biomech.* **18**, 247 (1985).
- [20] N.A.S. Affi, N.S. Gad, *Acta Mechanica* **149**, 229 (2001).
- [21] N.A.S. Affi, N.S. Gad, *Appl. Math. Comput.* **142**, 167 (2003).
- [22] N.S. Gad, *Appl. Math. Comput.* **217**, 4313 (2011).
- [23] M.T. Ouazzani, Ph.D. Thesis, Univ. Hassan II Casablanca, Morocco, 1991.
- [24] T. Hayat, E. Momoniat, F.M. Mahomed, *Math. Prob. Eng.* **2006**, 1 (2006).
- [25] K.S. Mekheimer, *Arabian J. Sci. Eng.* **30**, 69 (2005).
- [26] J.G. Bresseur, S. Corssin, *J. Fluid Mech.* **187**, 495 (1987).
- [27] A.R. Rao, S. Usha, *J. Fluid Mech.* **298**, 271 (1996).
- [28] A.H. Shapiro, M.Y. Jaffrin, S.L. Weinberg, *J. Fluid Mech.* **37**, 799 (1969).
- [29] H. Rachid, M.T. Ouazzani, *Int. J. Appl. Mech.* **6**, 1450061 (2014).